



Short Communication

Distinct view on batteries performance analysis

Moran Balaish^a, Alexander Kraysberg^b, Yair Ein-Eli^{a,b,*}^a The Nancy & Stephan Grand Technion Energy Program (GTEP), Technion-Israel Institute of Technology, Haifa 32000, Israel^b Department of Materials Science and Engineering, Technion-Israel Institute of Technology, Haifa 32000, Israel

ARTICLE INFO

Article history:

Received 23 June 2013

Received in revised form 26 August 2013

Accepted 27 August 2013

Available online 5 September 2013

Keywords:

Battery performance analysis

Integral average voltage

State of charge

Electrode reaction

Electrode structure

ABSTRACT

Many mathematical models have been developed for Li-battery cells performances. However, a critical need still do exists for a rather simple battery performance evaluation method. In the present study, such a parameter, Integral average voltage (IAV), is being introduced. Its utility, convenience and applicability are validated via existing experimental data derived from Li-air batteries and lithiated Ni doped Mn spinel 5 V cathode materials. IAV is simple to calculate using the cell charge/discharge profile; at the same time, it offers a perceptive analysis of cell features and associated processes.

© 2013 Elsevier B.V. All rights reserved.

1. Introduction

Li-related batteries are the most successful on the consumer electronic market; their usage is also gradually spreading to power sources for electric vehicles and energy storage for load levelling. Cost, safety, energy density and specific energy are the parameters, which are important for commercially viable and robust battery. Cell's discharge and charge voltages are both related to these parameters and thus, are among the most important cell characteristics. These parameters are important for practical battery applications [1] and are also particularly important in research and development (R&D) in the fields of battery chemistries and battery designs. In course of battery-related R&D works, cell's cathode and anode are usually being considered separately, assuming that $V_{\text{cell}} = V_a - V_c$ (V_a and V_c stands for anode and cathode potentials vs. a reference electrode, usually vs. Li^+/Li electrode).

Cell's over-voltage ΔV_{cell} , an additional important cell parameter, is defined as the difference between the electromotive force of the cell reaction $V_{\text{cell}}^{\text{emf}}$ and the actual cell voltage V_{cell} . The value ΔV_{cell} indicates the related energy loss in course of charge transfer reactions as well as the internal battery *ohmic* resistance. When it comes to comparison of cells with the same chemistry but with different electrode design as well as different electrolytes, it is accepted that an advantageous design provides the smallest values of ΔV_{cell} . The value ΔV_{cell} depends on the anode over-voltage ΔV_a

and cathode over-voltage ΔV_c , which are the differences between the actual electrode potential and the electromotive force of the anode V_a^{emf} and cathode V_c^{emf} reactions, respectively. The parameters V_{cell} and ΔV_{cell} depend generally on the charge being passed (Q), or the state of charge (SoC) [2,3] of the cell. Thus, all the above parameters are better to be denoted as $V_{\text{cell}}(Q)$, $\Delta V_{\text{cell}}(Q)$, $V_a(Q)$, $\Delta V_a(Q)$ and $V_c(Q)$, $\Delta V_c(Q)$. Fig. 1 illustrates for example, that these functions are diverse for different electrodes being utilized in Li-air battery design and therefore, a comparison of a particular battery design and chemistries in a selected SoC is rather quite difficult.

A possible solution for this problem is to compare electrodes and cells voltages at some (standardized) SoC; this approach resembles the industry-recommended method to measure cell's open circuit potential (OCP) after charge/discharge cycle at 4% of SoC [3]. The specific SoC value, which may be adopted, unavoidably is an arbitrary value. The example presented in Fig. 1 demonstrates that such approach may be quite confusing as SoC at a specific capacity of 0.5 Ah/g provides $\Delta V_c^{(I)} > \Delta V_c^{(II)}$ but SoC at 1 Ah/g is leading to inverse result as $\Delta V_c^{(I)} < \Delta V_c^{(II)}$.

2. Method of calculations

The obstacles described above may be overcome with the introduction of two new parameters: integral average cell (or electrode) voltage, $\overline{V_{\text{cell}}}$ and integral average cell (or electrode) over-voltage, $\overline{\Delta V_{\text{cell}}}$. These parameters can be implemented and applied both on discharging, as well as on charging processes evaluations. Specifically, the energy spent (or gained) in course of charge transfer through the potential difference $V_{\text{cell}}(Q_{\text{final}}) - V_{\text{cell}}(Q_{\text{initial}})$ is

* Corresponding author at: Department of Materials Science and Engineering, Technion-Israel Institute of Technology, Haifa 32000, Israel. Tel.: +972 4 829 4588; fax: +972 4 829 5677.

E-mail address: eineli@tx.technion.ac.il (Y. Ein-Eli).

$$E = \int_{Q_{\text{initial}}}^{Q_{\text{final}}} V(Q) dQ \quad (1)$$

Here, Q_{initial} stands for the charge of the cell at the beginning of the discharge (or charge) process, and Q_{final} stands for the charge of the cell at the end of the discharge (or charge) process.

Fig. 2 illustrates graphically Eq. (1), having the average integral voltage, over the $[Q_{\text{initial}}, Q_{\text{final}}]$ interval, being defined as:

$$\overline{V}_{\text{cell}} = \frac{\int_{Q_{\text{initial}}}^{Q_{\text{final}}} V(Q) dQ}{Q_{\text{final}} - Q_{\text{initial}}} = \frac{E}{\Delta Q} \quad (2)$$

The average over-voltage over this interval may be defined as:

$$\overline{V}_{\text{cell}} = \left| V_{\text{cell}}^{\text{emf}} - \overline{V}_{\text{cell}} \right| \quad (3)$$

When one electrode (cathode or anode) is being considered, the exact calculations can be individually implemented with each electrode; integral average electrode voltages and integral average electrode over-voltages maybe denoted as $\overline{V}_a, \Delta\overline{V}_a$ and $\overline{V}_c, \Delta\overline{V}_c$ for the anode and cathode, respectively.

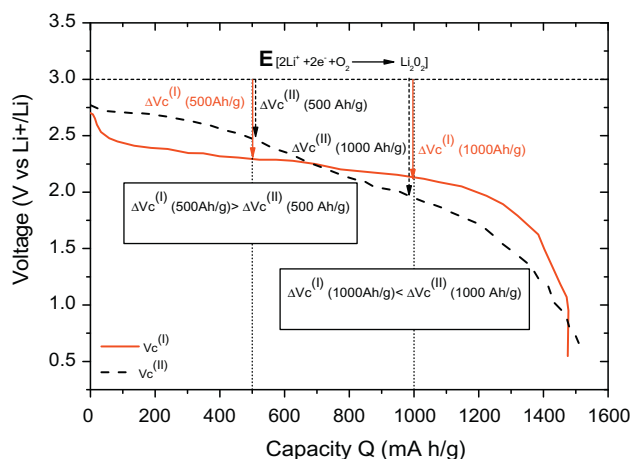


Fig. 1. Discharge profile curves of Li-air cathode – limited cells, air cathodes are made of different carbon materials; the cells operated in pure oxygen; curve (I) – solid red – is acquired from [4], $i = 0.1 \text{ mA/cm}^2$, super-P carbon black cathode, curve (II) is acquired from [5], $i = 0.2 \text{ mA/cm}^2$, meso-cellular carbon cathode. (For interpretation of the references to colour in this figure legend, the reader is referred to the web version of this article.)

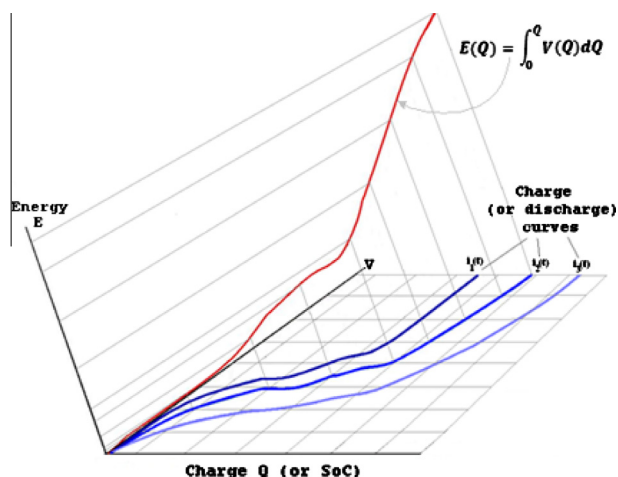


Fig. 2. Graphical representation of the cell (electrode) energy changes during charge (or discharge).

Routinely, the charge/discharge voltage and electrode over-voltage are of interest over the whole working interval. However, in a complete process, $Q_{\text{initial}} = 0$ and Q_{final} is the final cell capacity, Q_{full} ; on this basis, the integral average voltage and integral average over-voltage being presented below, are calculated over $[Q_{\text{initial}}, Q_{\text{final}}]$ interval.

3. The applicability of the proposed concept

The examples provided in this paper are based on a well-known literature data on oxide cathode materials, having a spinel structure, demonstrate the validity, convenience and robustness of the approach. LiMn_2O_4 spinel attracted an attention as possible cathode materials candidates for Li-ion batteries because of its high energy density and low cost. Since pure LiMn_2O_4 demonstrates low cyclability, current research is focused on the single- and double-doped spinels $\text{LiM}_x\text{Mn}_{2-x}\text{O}_4$ ($M = \text{Ni, Co, Cu, Cr, Fe, etc.}$), which have been reported to have operational voltages over 4 V, having an improved cycling performance, compared to pure LiMn_2O_4 [6–8]; the curves $V_{\text{cell}}(Q)$ for these oxides usually have a complicated shape and are inconvenient for comparison and further consideration, though.

A typical example of such research is the work of Singhal et al. [9], considering $\text{LiMn}_{2-x}\text{Ni}_x\text{O}_4$ spinels. The charge/discharge curves (shown in Fig. 3 [9]) demonstrate a strong dependence on Q , and in case of $x \neq 0$ the curves demonstrate two plateaus. Therefore, the curves are convenient only for qualitative consideration. The data presented in Fig. 3 were used for \overline{V}_c calculations, and the results are presented in Table 1 and in Fig. 4.

The average integral voltages \overline{V}_c , as presented in Table 1, better assist identifying several correlations between different variables and thus, allow a better comprehensive analysis of the studied electrode system. For example, Table 1 reveals that \overline{V}_c dependence on Ni content (x) correlates well with the dependence of Li partial intercalation energies on nickel content (Li partial intercalation energies resulted from ab initio quantum-mechanical calculations) [9]. It is remarkable that in course of cycling $\overline{V}_{c(x)}$ (charge) is practically unchanged, whereas $\overline{V}_{c(x)}$ (discharge) increases for $x > 0$. In order to discuss this feature; the following issues are to be considered.

First, Li^+ ion mobility has a major input on the cathode voltage [11]. Indeed, Li^+ ion migrates during charge within the Li-poor regions, from the oxide particle core toward the particle surface. Whereas, during discharge Li^+ ion migrates, vice versa, within the Li^+ -rich regions, from the surface toward the grain interior; it

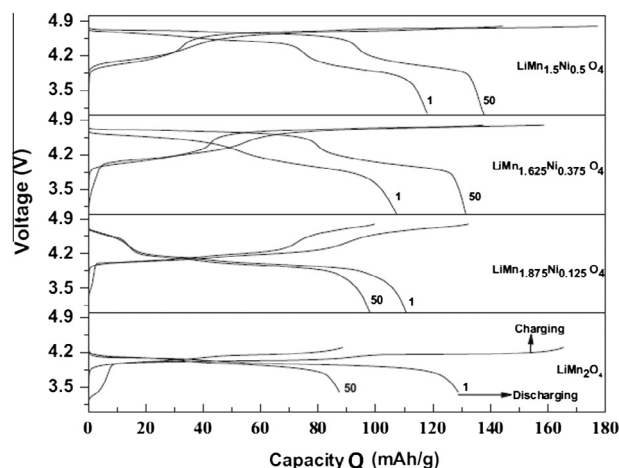


Fig. 3. Charge/discharge behaviour of $\text{LiMn}_{2-x}\text{Ni}_x\text{O}_4$ cycled in $\text{LiPF}_6 + (\text{EC} + \text{DMC})/\text{Li}$ coin cell (acquired from [9]).

Table 1

\overline{V}_c (discharge/charge), calculated using data from Fig. 3 and Eq. (2); the data were acquired using Grafula[®] curve tracking coder [10].

| Ni-content (x) | \overline{V}_c (discharge) 1st run (V) | \overline{V}_c (charge) 1st run (V) | \overline{V}_c (discharge) 50th run (V) | \overline{V}_c (charge) 50th run (V) | Li partial intercalation energy (eV) |
|----------------|------------------------------------------|---------------------------------------|-------------------------------------------|----------------------------------------|--------------------------------------|
| 0 | 3.941 | 4.042 | 3.94 | 4.054 | 4.31 |
| 0.125 | 4.027 | 4.288 | 4.24 | 4.3 | 4.54 |
| 0.375 | 4.196 | 4.5 | 4.42 | 4.5 | – |
| 0.5 | 4.288 | 4.576 | 4.43 | 4.57 | 4.8 |

was demonstrated that Li^+ -diffusion coefficient in Li^+ -rich regions is commonly lower than the coefficient values in Li^+ -depleted oxide regions [12,13], and thus, the (ionic) resistance along Li^+ -diffusion paths is higher during discharge. Hence, the grain *ohmic* voltage drop component of the total overvoltage is also expected to be higher during discharge. Second, considering $\text{LiMn}_{2-x}\text{Ni}_x\text{O}_4$ -oxides, the surface of the material is expected to lose manganese [14,15] in a process, which apparently results in near-surface oxide grain layers enrichment with nickel (for $x > 0$). Third, it is known that Li^+ -conductivity in $\text{LiMn}_{2-x}\text{Ni}_x\text{O}_4$ improves with increase in nickel content [9] and thus, the *ohmic* component is expected to diminish in course of cycling.

Overall, in course of cycling, the discharge overvoltage is diminishing and thus, the cell voltage $\overline{V}_{c(x)}$ (discharge) increases for $x \neq 0$, whereas since the charge overvoltage has smaller *ohmic* component, $\overline{V}_{c(x)}$ (charge) is not expected to experience a substantial change during cycling.

Another example of the validity and application of the Integral Average Voltage (IAV) concept is the analysis of the morphology of [oxide/binder/conductive additive] – cathode material. Namely, the electrochemical features of $\text{LiNi}_{0.4}\text{Mn}_{1.6}\text{O}_4$ – cathodes containing different content of conductive additives are presented in the work of Kunduraci et al. [16].

The discharge curves shown in Fig. 5 reveal that the rate capability of the cathode depends on the amount of conductive additive. It may be suggested that electrodes with low content of conductive additive suffer from a significant IR drop. These qualitative conclusions may be supported employing the concept of IAV.

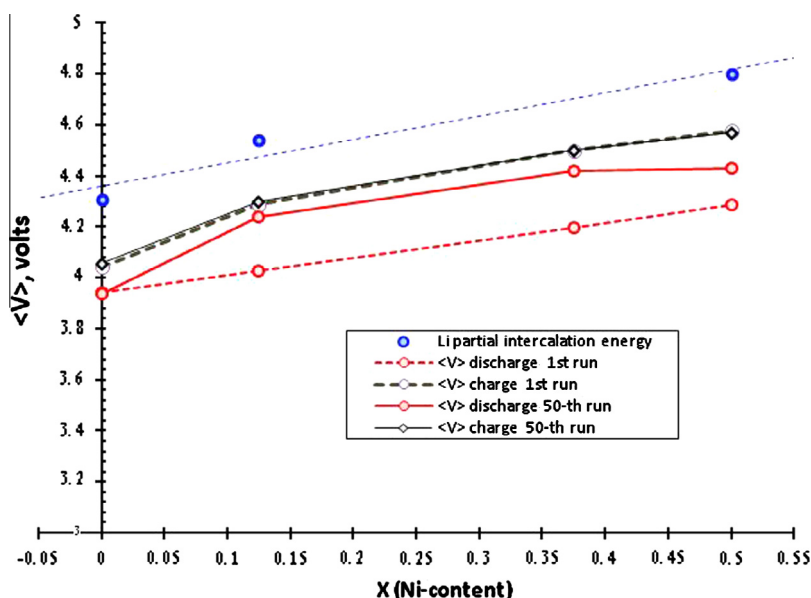


Fig. 4. $\overline{V}_{c(x)}$ (charge/discharge) for $\text{LiMn}_{2-x}\text{Ni}_x\text{O}_4/\text{LiPF}_6 + (\text{EC} + \text{DMC})/\text{Li}$ coin cell (data were acquired from [9] using Grafula[®] curve tracking coder [10], Li partial intercalation energies are also taken from [9]).

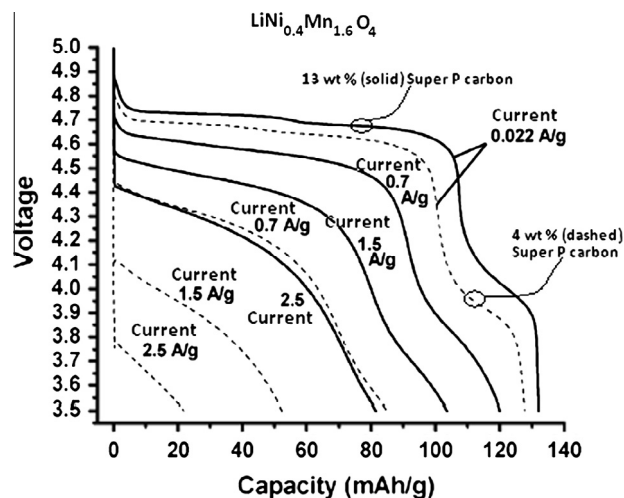


Fig. 5. Galvanostatic discharge voltage curves of $\text{LiNi}_{0.4}\text{Mn}_{1.6}\text{O}_4$ sample containing 4 wt.% (dashed) and 13 wt.% (solid) super P carbon as a conductive additive; the numbers on the graph represent the discharge current densities in A/g. Reprinted and modified with permission from Chem. Mater. 18 (2006) 3585–3592 [16]. Copyright 2006 Am. Chem. Soc.

Table 2 and Fig. 6 show \overline{V}_c (discharge) calculated from the data presented in Fig. 5.

Fig. 6 clearly demonstrates that the *ohmic* behaviour prevails for currents over 0.022 A/g for all conductive carbon contents. Also, expectably, the conductivity of the cathode containing 13% of carbon is 2.5 higher than the conductivity of the cathode utilizing only 4% of carbon.

The application of IAV is illustrated when Ni-substitution in high voltage spinel cathodes and different content of conductive additives in cathode materials is used. However, it is interesting to return to Fig. 1, demonstrating 2 different Li-air discharged cells, where the two cells possess different discharge profile (Curves I and II). As discussed earlier, Fig. 1 presents discharge profile curves of Li-air cells utilizing cathodes with different carbon materials (at different current densities). Curve (I) presents a better performance, as the operating voltage is constant over most of the charge

Table 2

\bar{V}_c (discharge) for $\text{LiNi}_{0.4}\text{Mn}_{1.6}\text{O}_4$ – cathode materials for different discharge currents and conductive additive content; the voltages are calculated using data from Fig. 5 and Eq. (2); data were acquired from Ref. [16] using Grafula® curve tracking coder [10].

| Current (A g^{-1}) | $V_c^{\text{discharge}}$ (V) 13% carbon | $V_c^{\text{discharge}}$ (V) 4% carbon |
|-------------------------------|-----------------------------------------|----------------------------------------|
| 0.022 | 4.55 | 4.44 |
| 0.7 | 4.32 | 4.11 |
| 1.5 | 4.2 | 3.84 |
| 2.5 | 4.09 | 3.53 |

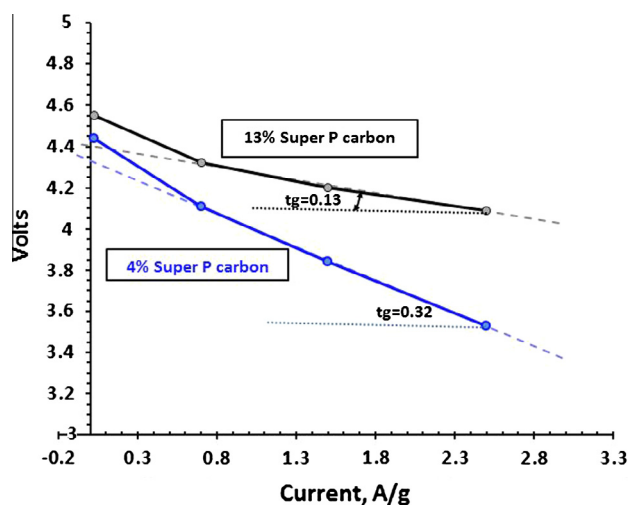


Fig. 6. \bar{V}_c (discharge) for $\text{LiNi}_{0.4}\text{Mn}_{1.6}\text{O}_4$ – cathode materials for different discharge currents and different conductive additive contents; data were acquired from Ref. [16] using Grafula® curve tracking coder [10].

passed. Indeed, the average voltage calculated according to IAV was 60 mV higher than the voltage calculated for Curve (II). Saying that, this dissimilarity does hardly represent the vast difference expressed clearly in the discharge curves. Thus, Fig. 1 is a classic example where IAV seems less suited to evaluate the cell voltage as the average does not necessarily represent the performance. Nevertheless, as Curve (II) presented two plateaus, indicating two electrochemical reactions, and the solid line showed only one plateau (the two discharge profile were acquired in different discharge current), it will be better suited if the IAV will be calculated up to 750 mA h/g and from 750 to 1500 mA h/g as per Curve (II). In this case, it will be noted that two main plateaus are distinguishable: $\bar{V}_c(0 - 750) = 2.52 \text{ V}$; $\bar{V}_c(750 - 1500) = 1.64 \text{ V}$, whereas in the case of Curve II (red bold line): $\bar{V}_c(0 - 1500) = 2.15 \text{ V}$.

4. Conclusions

The Integral Average Voltage (IAV) method is described and being evaluated; IAV provides a convenient and robust approach

presenting results of advanced Li metal cell (Li-air) and 5 V Li-ion positive electrode (lithiated Ni doped Mn spine) testing; it also allows a deeper understanding of electrode reactions and electrode structure. The method, if being adopted will be highly applicable and seems quite useful in battery-related research. IAV is proposed as a simple comparison tool applied to batteries with the same chemistry having different electrode designs. The validity and applicability of IAV is best illustrated when one constituent in the active materials is being modified. For example, IAV application is mostly effective in the evaluation of different content of Ni-substitutions in high voltage spinel cathodes or different content of conductive additives in the electrode materials. IAV is a good parameter, replacing the nowadays random voltage determination. This simple calculation is applicable to numerous kinds of batteries, but as in the case of every other parameter, the researcher must not ignore common sense and logic, before implementing IAV.

Acknowledgments

This research was partially financially supported by The Nancy & Stephan Grand Technion Energy Program (GTEP), Israel Science Foundation (ISF), the Israeli Ministry of Energy and Water Resources and Israel National Research for Electric Propulsion (INREP).

References

- [1] M.E. Manna, Battery Design Guide for Portable Electronics – An Approach in Simple Terms, Ultralife Corporation. <<http://ultralifecorporation.com/download/207/>>.
- [2] S. Piller, M. Perrin, A. Jossen, J. Power Sour. 96 (2001) 113–120.
- [3] V. Pop, H.J. Bergveld, J.H.G. Op he velt, P.P.L. Regtien, D. Danilov, P.H.L. Notten, Battery Management Systems: Accurate State-of-Charge Indication for Battery Powered Applications, vol. 9, Springer Verlag, 2008.
- [4] J. Read, J. Electrochem. Soc. 149 (2002). A1190.
- [5] X. Yang, P. He, Y. Xia, Electrochem. Commun. 11 (2009) 1127–1130.
- [6] R. Santhanam, B. Rambabu, J. Power Sour. 195 (2010) 5442–5451.
- [7] J.B. Goodenough, Y. Kim, Chem. Mater. 22 (2009) 587.
- [8] B. Xua, M.-Che Yang, Y.S. Meng, Meet. Abstr. – Electrochem. Soc. 1002 (2010).
- [9] R. Singhal, J. Saavedra-Aries, R. Katiyar, Y. Ishikawa, M.J. Vilkas, S.R. Das, M.S. Tomar, R.S. Katiyar, J. Renew. Sust. Energy 1 (2009) 023102/1–023102/11.
- [10] Copyright © Mr.WESIK Version v2.10 24/10/2001, (acquired 10-2011). <http://www.4shared.com/get/6SeK55iD/grafula3_curve_tracking.html>.
- [11] M.A. Roscher, J. Vetter, D.U. Sauer, J. Power Sour. 191 (2009) 582–590.
- [12] A. Van der Ven, G. Ceder, Solid-State Lett. 3 (2000) 301–304.
- [13] D. Morgan, A. Van der Ven, G. Ceder, Electrochem. Solid-State Lett. 7 (2004) A30–A32.
- [14] J.W. Fergus, J. Power Sour. 195 (2010) 939–954.
- [15] L.-Wen Ma, B.-Zhen Chen, X.-Chang Shi, W. Zhang, K. Zhang, Colloids Surf. 369 (2010) 88–94. A.
- [16] M. Kunduraci, J.F. Al-Sharab, G.G. Amatucci, Chem. Mater. 18 (2006) 3585–3592.